http://dx.doi.org/10.14500/aro.11097

Structural and Optical Properties of Cadmium Sulfide-doped Silver Deposited on Glass and Polymer Substrates by Chemical Spray Pyrolysis

Niaz H. Hamad, Mohammad G. Faraj, and Akram H. Taha

Department of Physics, Faculty of Science and Health, Koya University,
Koya, KOY45, Kurdistan Region – F.R. Iraq

***Abstract*—This process of this paper is carried out using the chemical spraying method to produce homogeneous thin films of pure cadmium sulfide-doped with silver at different percentages of 1%, 3%, and 5% on glass and polyimide plastic substrates at 300°C. The aim is to study the optical and structural properties of the samples and the effect of the silver doping rate on films produced with these properties. Due to X-ray diffraction studies, all films created had a hexagonal phase, and it was noticed that they had a very precise structure free of holes or cracks. The obtained crystal size ranged between 22.74 nm and 55.05 nm for different substrates, and the prominent plane was (002). From the optical properties, all films exhibited transmission higher than 60%, thus showing a low absorption, which makes them be used as light-permeable layers in the Solar Cell system. In addition, emission peaks were revealed by photo luminescence spectra examination at wavelengths ranging between (542.94 nm) and (546.02 nm), which led to calculate the energy gap (E_g). of the produced films, ranged between (2.27 eV) and (2.28 eV) for the different substrates.**

***Index Terms*—Cadmium sulfide-*Ag*, Chemical spray technique, X-ray diffraction pattern, Photo luminescence studies.**

I. Introduction

Recent advances in thin film nanotechnology (Ahmed, et al., 2021b) offer a possible method for solar energy applications to lessen the environmental crisis brought on by energy use. Because solar energy is one of the most significant renewable energy sources, scientists have created or modified several semiconductor thin films to optimize high solar cell efficiencies at cheap cost (Ahmed, et al., 2020). Due to its broad bandgap (2.42 eV) at ambient temperature, chalcogenides of cadmium, notably cadmium sulfide (CdS), are one of the most actively researched topics among material scientists (Islam, et al., 2013, Shkir, et al., 2020c). The II-VI semiconductor family such as (CdS) has received much attention for its tunable optical and electrical properties (Mahmood, et al., 2018, Shkir, et al., 2020d).

Bulk CdS, one of the most significant window layer materials for solar cell devices, typically transmits energy in the low energy region of the visible solar spectrum. However, by adding a suitable amount of impurity, particularly transition metal ions, it is possible to re-engineer CdS to transmit the entire visible spectrum. Due to their capacity to alter the bandgap, noble metals, including gold (*Au*), copper (*Cu*), and silver (*Ag*), have been regarded as the most promising possibilities among these (Bora, et al., 2021) and reduce resistivity while also produce structural changes. A crucial factor for solar cell window layer materials is low resistance and good transmission when combined with p-type semiconductor absorber thin films such as *CdTe*, Cu_2S (Ojeda-Barrero, et al., 2018), $CuInSe_2$ (Rahman, Hossain and Ismail, 2020), *CdSe*, and PbS (Aboud, et al., 2019). CdS is well known for its n-type wide band gap, which makes it an appropriate window layer counterpart for solar cell applications (Manthrammel, et al., 2020, Nazir, et al., 2014).

Thus, CdS has wide applications in optoelectronic device technologies, including optical filters, LEDs (Ahmed, et al., 2021a), lasers (Ikhmayies, 2020), photocatalysis (Manthrammel, et al., 2020), photodetectors (Mohammed, et al., 2021), nonlinear integrated optical devices (Rahman, Hossain and Ismail, 2020), and multicolor optical switches (Shkir, et al., 2020b).

A novel feature of the ongoing work is the fabrication and characterization of films fabricated on polyimide (PI) plastic substrates using chemical spray pyrolysis techniques with varying Ag ratios. In this respect, the use of flexible polymer substrates is of great interest (Faraj, Ibrahim and Salhin Ali, 2012, Faraj, Pakhuruddin and Taboada, 2017). It has important advantages such as light weight, high impact resistance, and scalable roll-to-roll manufacturing process.

Many methods are employed to prepare CdS thin films, including vacuum evaporation (Shaban, et al., 2021), chemical deposition (Shkir, et al., 2020b), sputtering (Yadav, Barote and Masumdar, 2010), successive ionic layer adsorption and reaction (SILAR) (Deshmukh, Kheraj and

ARO-The Scientific Journal of Koya University
Vol. XI, No. 1 (2023), Article ID: ARO.11097. 6 pages
DOI: 10.14500/aro.11097
Received: 23 October 2022; Accepted: 07 January 2023
Regular research paper: Published: 15 January 2023
Corresponding author's e-mail: niazhamakhan25@gmail.com

Panchal, 2018, Taghizadeh Chari and Fadavieslam, 2019), printing (An, et al., 2021), laser ablation (Wada, 2022), electrodeposition (Valencia and Baena, 2015), chemical bath techniques (Kakhaki, et al., 2022), solgel (Mohammed, et al., 2021), and chemical spray pyrolysis CSP (Vishwas, Shamala and Gandla, 2022). The characteristics of thin films and powders of CdS at the nanoscale depend on the dopant type, concentration, method of preparation/deposition, and pH application (Shkir, et al., 2020a).

In the present work, CdS and CdS -Ag thin films were fabricated with a chemical spray pyrolysis method and deposited on different substrates, glass, and PI plastic, with different ratios of doping. A comparative study of the optical properties before and after Ag layer deposition on the surface of the CdS has been performed, highlighting the strong reduction in the energy gap and increase in transmission.

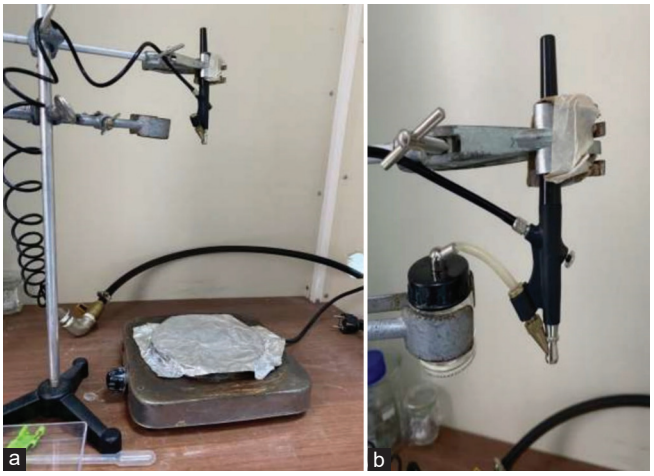

Fig. 1. (a) Spray pyrolysis technique. (b) The amplified section of the device.

II. Experimental Procedure

A. Preparation of CdS Solutions

A thermal chemical spraying solution of CdS was prepared first without doping and then by doping with different weight ratios (1%, 3%, and 5%) of silver with molar weights of cadmium chloride and silver nitrate to obtain the mentioned ratios. The weight of each of the cadmium chlorides ($CdCl_2.H_2O$) $\left(CdCl_2.H_2O\right)$ was approximately 0.91653 g (as a source of cadmium ions), and thiourea [$(NH_2)_2CS$]. Approximately 0.38032 g (source of sulfur ions) to obtain (CdS). The solutions are reacted according to (1) to obtain (CdS) doped with silver, silver nitrate with masses (0.0129, 0.3878, and 0.0648) g was used to obtain the ratios mentioned above. All solutions were prepared with a fixed titer of molarities of (0.1 M). All weights were wholly dissolved in distilled water in a 250 mL volumetric vial. Then, the mixture was mixed well at a temperature slightly more significant than room temperature with sufficient times using a magnetic stirrer to obtain a clear, suspended liquid. The solutions are reacted to (2):

$$CdCl_2 + (NH_2)_2CS + 3H_2O \rightarrow CdS \downarrow + 2NH_4Cl + CO_2 \uparrow \quad (1)$$

$$AgNO_3 + H_2O \rightarrow Ag \downarrow + H_2 \uparrow + NO_2 \uparrow \quad (2)$$

All the products of the above reactions are gases except for CdS and Ag, which are impurities.

B. Substrate Cleaning

The substrates used in this paper are glass and PI plastic, which were cleaned using methanol solution and immersed in it for more than 15 min to eliminate contaminants. The substrate was cleaned with distilled water after cleaning (DI water). This was followed by drying with warm, dry air.

C. Experience

After many attempts using chemical spray pyrolysis technique, a device used is shown in Fig. 1a and b, and the following optimization conditions were noticed: the substrate temperature was kept at 300°C. During deposition, the distance between the nozzle and the substrate was approximately 29 cm, the deposition rate time was approximately (3–5) s, the spraying rate was 1 spray, and the carrier gas was air. The above-mentioned solutions were sprayed on different substrates with the weight mentioned above ratios. The obtained films were adherent.

III. Characterization Technique

X-ray diffraction (XRD) analysis (PANalytical-Typenr: 94 30 060 03002-S/N: DY1376-MFG) Technique was used to study and investigate the structural properties of thin film models. An X-ray diffractometer was used with a wide diffraction angle (2Θ) range of (5°-80°) degrees. (UV–VIS) double beam spectrometer of type (PerkinElmer precisely Lambda 25-Shelton, CT 06484 USA-Part No. L600000B-Serial No. 101N8022902) was also used to determine and measure the optical transmittance in the wavelength range of 400 and 800 nm. Finally, a photo luminescence (PL) device (instrument Cary Elipse-instrument serial number: MY131500007) with an excitation wavelength of fluorescein (400 nm) was used to calculate the direct energy gap of the film.

IV. Results and Discussion

A. Structural Studies

The crystal structures of CdS and Ag-doped thin films on different substrates were investigated using XRD. Moreover, in both cases the thin films were deposited on glass and PI substrates. The prominent 2θ peaks are shown in Table I for glasses and PI substrates.

The prominent peaks for the sample CdS pure on the glass substrate marked in Fig. 2 are 24.87°, 26.53°, 28.25°, 36.64°, 43.86°, and 48.08°, with the corresponding diffraction planes (100), (002), (101), (110), (103), and (113). This is the same for the CdS doping Ag ratios, with the difference shown in Fig. 2 due to the different impurity percentages. The mean

http://dx.doi.org/10.14500/aro.11097

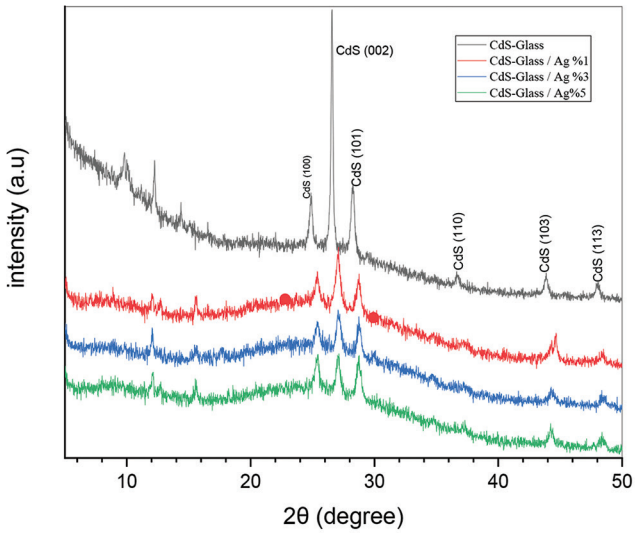

Fig. 2. X-ray diffraction patterns of cadmium sulfide and Ag-doped thin films deposited on glass substrates.

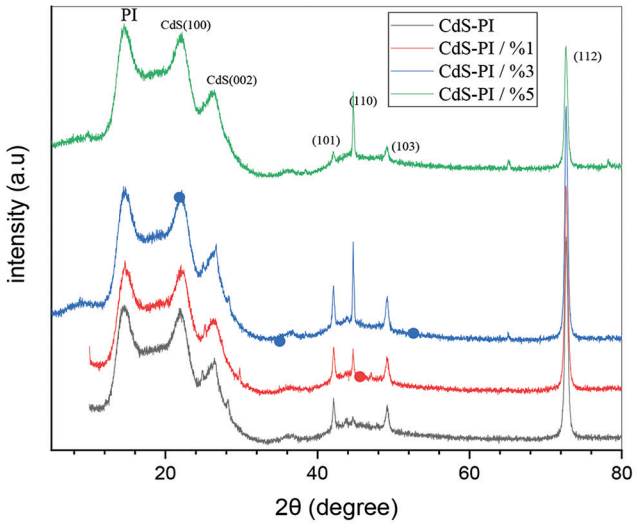

Fig. 3. X-ray diffraction pattern of cadmium sulfide and Ag-doped thin film deposited on polyimide substrate.

peak is 26.53°, and its corresponding plane is (002), roughly the same as the other samples. These measured diffraction peaks are highly in agreement with the standard XRD data of JPDS (Card no. 41–1049) for hexagonal wurtzite structures and indicate the formation of CdS films with those structures, as reported in (Mahmood, et al., 2018, Yang, et al., 2018). However, the prominent peaks for the sample CdS pure on the PI substrate marked in Fig. 3 had six diffraction peaks at 2θ values of 22.11°, 26.43°, 42.10°, 44.63°, 49.16°, and 72.43° corresponding to their diffraction planes (100), (002), (101), (110), (103), and (112). This is the same for CdS doping of Ag on PI, with the difference due to the different impurity percentages, as shown in Fig. 3. The mean peak in Fig. 3 is 26.43°, and its corresponding plane is (002), roughly the same as the other samples. These diffraction peaks support the conventional XRD data JCPD6-314 for hexagonal wurtzite structures, which indicate the formation of CdS films with such structures as reported in (Faraj, Pakhuruddin and Taboada, 2017, Mensah, et al., 2021), in which hexagonal-structured thin films are preferred for solar cell applications (Taghizadeh Chari and Fadavieslam, 2019). In both cases, by comparing the above data in Figs. 2 and 3, there is a difference between the peaks obtained due to the different substrates. The average crystallite size was estimated from the X-ray diffraction pattern using the prominent peak, depending on Scherrer's equation:

$$D = \frac{0.9\lambda}{\beta \cos\theta} \quad (3)$$

Where D is the crystallite size, λ is the X-ray wavelength (1.54 A°), β is the full width at half maximum (FWHM) in radians, and θ is the center of the diffraction peak angle value in radians. The FWHM value (2 θ) and peaks were calculated using the XRD data peak program, as shown in Table I.

With the use of Scherrer's formula, the particle size values are determined. Compared to natural crystallite sizes, the value derived from Scherrer's equation is different. In XRD analysis, peak broadening often results from physical parameters such as crystallite size and lattice strain as well as instrumental broadening. Physical factors are represented by the FWHM of each diffraction peak as a linear combination of the contributions from lattice strain and crystallite size calculated using Scherrer's equation and the actual crystallite size. Table 1 lists the parameters, which are different, and it has been found that unit cell size increases for some samples and decreases for others with increasing concentrations of Ag in CdS. As the unit cell decreases evident volume, this confers a suggestion regarding incorporating Ag dopant in CdS matrix or due to intrinsic defects. This may also be explained by Vegard's law (Shkir, et al., 2020a). Vegard's law states that if doping takes place at interstitial or substitutional positions in the matrix, the lattice will increase or decrease, respectively. Hence, both possibilities exist.

TABLE I
Crystal Size and (2θ) for CdS Pure and Ag-Doped on PI and Glass Substrates

Sample	(2θ) degree	FWHM	D nm
CdS -Glass	26.53	0.12	55.05
CdS -Glass-Ag 1%	27.06	0.25	37.17
CdS -Glass-Ag 3%	27.06	0.25	37.17
CdS -Glass-Ag 5%	27.12	0.17	55.05
CdS pure-PI	27.12	0.17	55.05
CdS -PI-Ag 1%	25.19	0.15	65.77
CdS -PI-Ag 3%	26.68	0.17	55.01
CdS -PI-Ag 5%	26.40	0.40	22.7

CdS: Cadmium sulfide, PI: Polyimide

B. Optical Characterization

UV-visible spectra

Figs. 4 and 5 show the optical transmission spectra of the CdS thin films with varying Ag ratios on glass and PI substrates. All the films show more than 60% transmission for wavelengths longer than 500 nm. As the Ag ratios increased, the sample optical transmittance increased within

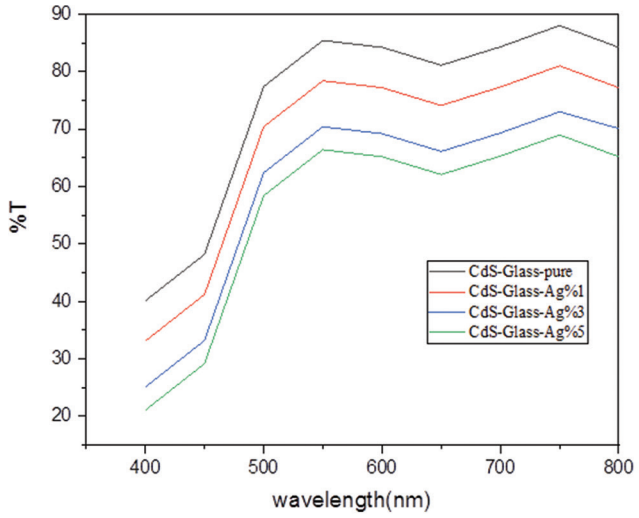

Fig. 4. Transmission spectra of cadmium sulfide pure and Ag-doped with ratios of (1%, 3%, and 5%) on a glass substrate.

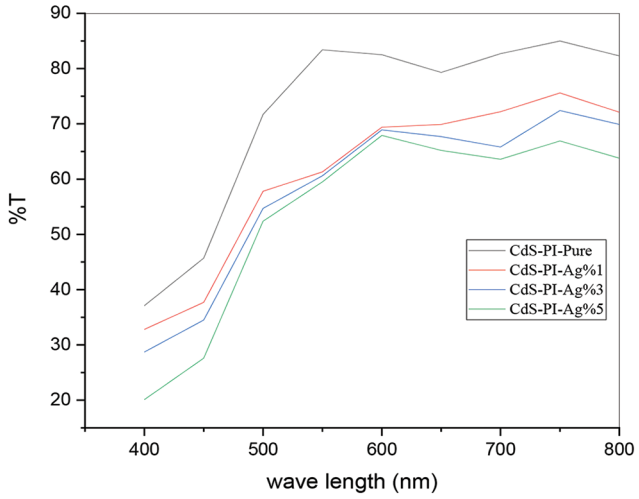

Fig. 5. Transmission spectra of cadmium sulfide pure and Ag-doped doped with ratios of (1%, 3%, and 5%) on polyimide substrate.

a (400–800) nm wavelength region. In the CdS films, the optical transmittance spectra increased as the Ag doping ratios increased. This occurred because the addition of silver enhanced the crystal structure and reduced surface roughness; similar behavior in the transmission spectra of the CdS films has been reported in (Manthrammel, et al., 2020). Thus, showing a low absorption, it can be used as a light-permeable layer in the Solar Cell system.

PL studies

PL studies help understanding the various transitions inside the samples when light incident on. Because of the vacancies of Cd and S and the interstitial locations of Cd and S, CdS is well known for its wide emission spectra in the UV, blue, green, yellow, and red spectra. According to reports in (Manthrammel, et al., 2020), these inherent flaws may function as luminous centers and provide a wide defect allied PL spectrum. Figs. 6 and 7 represent the PL spectra of CdS pure and doped Ag with different weight ratios on

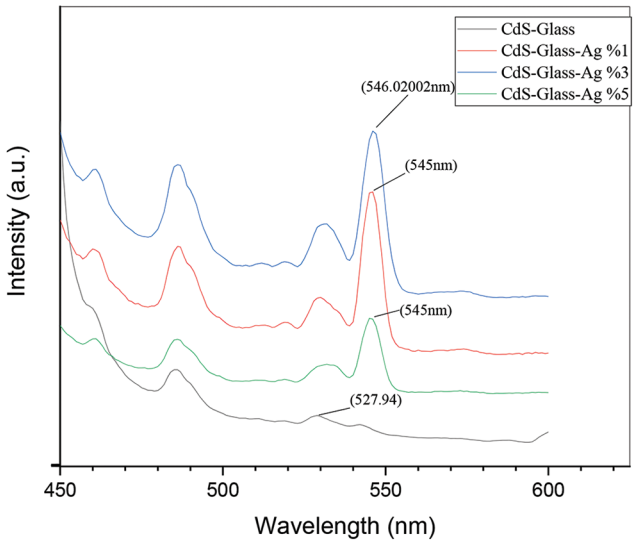

Fig. 6. Cadmium sulfide photo luminescence spectra and Ag-doped with different concentrations on a glass substrate.

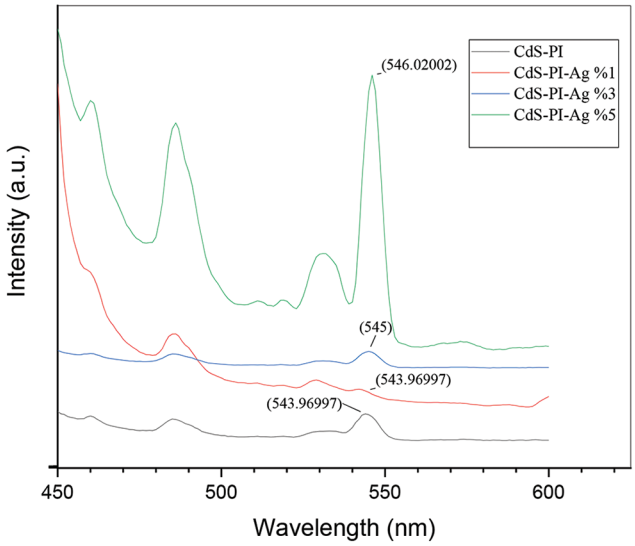

Fig. 7. Cadmium sulfide photo luminescence spectra and Ag-doped with different concentrations on polyimide substrate.

glass and PI substrates at constant temperature 300°C. Thin films excited at 400 nm. The intense peak in both cases is the glass substrate and polyamide plastic, and in all models, it ranges from 542.94 nm to 546.02 nm, see Fig. 6, Fig. 7 and recorded in Table II. Other weak peaks appear in the Figs. 6 and 7, and these weak peaks indicate the transition from one band to another and that the emission is related to defects. However, it is also noticed that the values of the wavelengths of the models change slightly change the long wavelengths due to the increase in the doping ratio, which indicates that the defect level is due to low interstitial defects. As the wavelength increases, the frequency decreases, so the energy gap decreases, and this is proportional to the facts as in (Ikhmayies, 2020). To calculate the energy gap, based on Planck's law in all models, used (4), and the results are recorded in Table II.

http://dx.doi.org/10.14500/aro.11097

TABLE II
ENERGY GAP FOR CDS PURE AND AG-DOPED WITH DIFFERENT CONCENTRATIONS ON GLASS AND PI SUBSTRATES

Sample	Wavelength (nm)	Energy gap (eV)
CdS-Glass	527.94	2.34
CdS-Glass-Ag 1%	545	2.27
CdS-Glass-Ag 3%	546.02	2.27
CdS-Glass-Ag 5%	545	2.27
CdS pure-PI	543.97	2.27
CdS-PI-Ag 1%	543.97	2.27
CdS -PI-Ag 3%	545	2.27
CdS -PI-Ag 5%	546.02	2.27

CdS: Cadmium sulfide, PI: Polyimide

$$E_g = h\nu \quad (4)$$

Where E_g is the energy gap in a unit (eV), h is Planck's constant (6.63×10^{-34} *J.s*) and ν is the frequency of visible light in *Hz*. $\nu = \frac{c}{\lambda}$ where c is $\left(3\times10^8 \frac{m}{s}\right)$. λ is the visible light wavelength in nm.

Then, equation (4) can be reformed as:

$$E_g = \frac{1240}{\lambda_{nm}} \text{ (eV)} \quad (5)$$

The energy gap was calculated according to (5). The energy gap values show that they are 2.34 eV and 2.27 eV for pure CdS samples in glass and PI plastic substrates, respectively. A very small difference is observed between them, perhaps due to the different substrates. Since the theoretical E_g value of CdS is 2.42 eV, compared with the practical results, a slight difference between them is found at approximately 0.08 eV. This may be due to film deposition.

For the other samples, which were impregnated with silver in different proportions, in both cases, the glass substrates and polyamide plastics showing clear differences in the value of the energy gap, as recorded in Table II. As the percentage of doping increases, the value of the energy gap decreases, which makes CdS films used in solar cells and leads to an increase in electrical conductivity and ease to charge carriers, moving quickly from the valence band to the conduction band by absorbing less energy from visible light, which approaches the color of yellow as acceptable with advance reports (Shkir, et al., 2020a).

V. Conclusion

Recent studies on the CdS deposition method using chemical spray pyrolysis and CdS doped Ag thin films onto glass have attracted much attention because of its low cost, ease of use, and capacity for mass production. In this study, CdS thin films were deposited by chemical spray pyrolysis onto glass and PI substrates at various Ag ratios (1%, 3%, and 5%). Following deposition, the effect of the Ag ratio on the structure and film optical properties was studied. The XRD pattern confirmed the proper phase formation of the films. The crystalline size varied between 22.74 nm and 55.05 nm. The optical transmissions of all films were <60% for wavelengths longer than 500 nm. The CdS film optical transmittance spectra increased as the Ag doping ratios increased. The energy band gap of all films was determined by PL measurement. The values ranged between 2.27 eV and 2.28 eV.

Acknowledgment

The authors would like to thank Koya University for the permission granted to conduct their research activities.

References

Aboud, A.A., Mukherjee, A., Revaprasadu, N., and Mohamed, A.N., 2019. The effect of Cu-doping on CdS thin films deposited by the spray pyrolysis technique. *Journal of Materials Research and Technology*, 8(2), pp.2021-2030.

Ahmed, A.A.A., Al-Hesni, N.M., Al-Osta, A.H., Al-Salmi, M.L., Manssor, K.A., Ja'adan, S.M., Al-Asbahi, B.A., Qaid, S.M.H., Ghaithan, H.M., and Farooq, W.A., 2021a. Influence of single and dual doping (Ag and Co) on the optical properties of CdS quantum dot thin films for solar application. *Optik*, 246, p.167824.

Ahmed, M.A., Ahmed, E.H., Sabri, M.M., and Abed, W.R., 2020. The performance of high-efficiency perovskite solar cell (PSC) by using capacitance simulator. *Journal of Physics Conference Series*, 1530, p.012149.

Ahmed, M.A., Sabri, M.F.M., and Abed, W.R., 2021b. The study of optical and electrical properties of nanostructured silicon carbide thin films grown by pulsed-laser deposition. *Aro Scientific Journal of Koya University,* 9(2), pp.46-50.

An, B.G., Kim, H.R., Chang, Y.W., Park, J.G., and Pyun, J.C., 2021. Photosensors-based on cadmium sulfide (CdS) nanostructures: A review. *Journal of the Korean Ceramic Society,* 58(6), pp.631-644.

Bora, J., Borthakur, A., Arandhara, G., and Saikia, P.J., 2021. Effect of Ag doping on the optical and structural properties of CdS/polyvinyl alcohol thin films by thermolysis process. *Thin Solid Films,* 734(2), p.138847.

Deshmukh, S.G., Kheraj, V., and Panchal, A.K., 2018. Preparation of nanocrystalline CdS thin film by successive ionic layer adsorption and reaction (SILAR) method. *Materials Today Proceedings,* 5(10), pp.21322-21327.

Faraj, M.G., Ibrahim, K., and Salhin Ali, A., 2012. Fabrication and characterization of thin-film Cu (In, Ga) Se2 solar cells on a PET plastic substrate using screen printing. *Materials Science in Semiconductor Processing*, 15(2), pp.165-173.

Faraj, M.G., Pakhuruddin, M.Z., and Taboada, P., 2017. Structural and optical properties of cadmium sulfide thin films on flexible polymer substrates by chemical spray pyrolysis technique. *Journal of Materials Science Materials in Electronics*, 28(9), pp.6628-6634.

Ikhmayies, S.J., 2020. *Advances in Energy Materials*. 1 st ed., Springer International Publishing, United States of America.

Islam, M.A., Hossain, M.S., Aliyu, M.M., Chelvanathan, P., Huda, Q., Karim, M.R., Sopian, K., and Amin, N., 2013. Comparison of structural and optical properties of CdS thin films grown by CSVT, CBD and sputtering techniques. *Energy Procedia*, 33, pp.203-213.

Kakhaki, Z.M., Youzbashi, A.A., Sangpour, P., Naderi, N., and Orooji, Y., 2022. Influence of Cd salt concentration on the photoconductivity of CdS thin films prepared by chemical bath technique. *Materials Science in Semiconductor Processing*, 148, p.106773.

Mahmood, W., Ali, J., Thomas, A., Awan, S.U., Jackman, M., Haq, A.U., Hassan, M.U., and Shah, N.A., 2018. Role of Ag^{1+} substitutional defects on the electronic and optical properties of n-type CdS thin films semiconductor for sustainable and stable window layer in solar cells technology. *Optical Materials*, 85, pp.143-152.

Manthrammel, M.A., Shkir, M., Shafik, S., Anis, M., and Alfaify, S., 2020. A systematic investigation on physical properties of spray pyrolysis-fabricated CdS thin films for opto-nonlinear applications: An effect of Na doping. *Journal*

of Materials Research, 35(4), pp.410-421.

Mensah, M.B., Awudza, J.A., Revaprasadu, N., and O'brien, P., 2021. Synthesis of CdS and PbS nanoparticles by the thermal decomposition of ethyl xanthate complexes in castor oil using the heat-up technique. *Materials Science in Semiconductor Processing*, 122, p.105493.

Mohammed, I.M.S., Gubari, G.M.M., Sonawane, M.E., Kasar, R.R., Patil, S.A., Mishra, M.K., Kutwade, V.V., and Sharma, R., 2021. Influence of pH on the physical properties of CdS thin film and its photosensor application. *Applied Physics A*, 127(8), p.597.

Nazir, A., Toma, A., Shah, N.A., Panaro, S., Butt, S., Sagar, R.R., Raja, W., Rasool, K., and Maqsood, A., 2014. Effect of Ag doping on opto-electrical properties of CdS thin films for solar cell applications. *Journal of Alloys and Compounds*, 609, pp.40-45.

Ojeda-Barrero, G., Oliva-Avilés, A., Oliva, A., Maldonado, R.D., Acosta, M., and Alonzo-Medina, G.M., 2018. Effect of the substrate temperature on the physical properties of sprayed-CdS films by using an automatized perfume atomizer. *Materials Science in Semiconductor Processing*, 79, pp. 7-13.

Rahman, M.F., Hossain, J., and Ismail, A.B., 2020. Structural, surface morphological and optical properties and their correlation with the thickness of spin coated superior quality CdS thin film synthesized using a novel chemical route. *SN Applied Sciences*, 2(12), p.1956.

Shaban, Z.M., Khlati, J.A., Khadayeir, A.A., Habubi, N.F., and Chiad, S.S., 2021. Structural, morphology and optical properties of Ag-doped nanostructured CdS thin films. *Journal of Physics Conference Series*, 1999(1), p.012063.

Shkir, M., Ashraf, I.M., Alfaify, S., El-Toni, A.M., Ahmed, M., and Khan A., 2020a. A noticeable effect of Pr doping on key optoelectrical properties of CdS thin films prepared using spray pyrolysis technique for high-performance photodetector applications.*Ceramics International*, 46(4), pp.4652-4663.

Shkir, M., Ashraf, I.M., Chandekar, K.V., Yahia, I.S, Khan, A., Algarni, H., and Alfaify, S., 2020b. A significant enhancement in visible-light photodetection properties of chemical spray pyrolysis fabricated CdS thin films by novel Eu doping concentrations. *Sensors and Actuators A Physical*, 301, p.111749.

Shkir, M., Ashraf, I.M., Khan, A., Khan, M.T., El-Toni, A.M., Alfaify, S., 2020c. A facile spray pyrolysis fabrication of Sm: CdS thin films for high-performance photodetector applications. *Sensors and Actuators A Physical*, 306, p.111952.

Shkir, M., Khan, Z.R., Anis, M., Shaikh, S.S., and Alfaify, S., 2020d. A comprehensive study of opto-electrical and nonlinear properties of Cu@ CdS thin films for optoelectronics. *Chinese Journal of Physics*, 63, pp.51-62.

Taghizadeh Chari, F., and Fadavieslam, M.R., 2019. Microstructural, optical and electrical properties of CdS thin films grown by spray pyrolysis technique as a function of substrate temperature. *Optical and Quantum Electronics*, 51(2), pp.1-16.

Valencia, D.E.J., and Baena, O.J.R., 2015. Portland cement clinker formation: High temperature equilibria and phase composition prediction. In: *TMS 2015 144th Annual Meeting and Exhibition*. Springer, Germany. pp.879-886.

Vishwas, M., Shamala, K.S., and Gandla, S., 2022. Comparison of optical properties of CdS thin films synthesized by spray pyrolysis and thermal evaporation method. *Journal of Optics*, 51(1), pp.1-5.

Wada, H., 2022. Preparation of functional nanoparticles by laser process in liquid and their optical applications. In: *High-energy Chemistry and Processing in Liquids*. Springer, Germany. pp.237-259.

Yadav, A.A., Barote, M.A., and Masumdar, E.U., 2010. Studies on nanocrystalline cadmium sulphide (CdS) thin films deposited by spray pyrolysis. *Solid State Sciences*, 12(7), pp.1173-1177.

Yang, F., Tian, X., Zhang, K., Zhang, X., and Liu, L., 2018. The morphology-property effect and synergetic catalytic effect of cds as electrocatalysts for dyesensitized solar cells. *ECS Journal of Solid State Science and Technology*, 7, pp.311-316.